

Noise Mitigation of Drone by Modifying Propeller Blade

M.Tech Thesis

by

KARTIK MADHUKAR PATIL



**DEPARTMENT OF MECHANICAL ENGINEERING
INDIAN INSTITUTE OF TECHNOLOGY INDORE**
JUNE 2025

Noise Mitigation of Drone by Modifying Propeller Blade

A THESIS

*Submitted in partial fulfillment of the
requirements for the award of the degree*

of

Master of Technology

by

KARTIK MADHUKAR PATIL



**DEPARTMENT OF MECHANICAL ENGINEERING
INDIAN INSTITUTE OF TECHNOLOGY INDORE**
JUNE 2023



CANDIDATE'S DECLARATION

I hereby certify that the work which is being presented in the thesis entitled "**Noise Mitigation of Drone by Modifying Propeller Blade**" in the partial fulfilment of the requirements for the award of the degree of **MASTER OF TECHNOLOGY** and submitted in the **DEPARTMENT OF MECHANICAL ENGINEERING, Indian Institute of Technology Indore**, is an authentic record of my own work carried out during the time period from June 2024 to May 2025 under the supervision of **Prof. Anand Parey**, Professor, Department of Mechanical Engineering, Indian Institute of Technology Indore and **Dr. Krishna Mohan Kumar**, Assistant Professor, Department of Mechanical Engineering, Indian Institute of Technology Indore.

The matter presented in this thesis has not been submitted by me for the award of any other degree of this or any other institute.

Kartik Patil
16/06/2025

Signature of the student with date
(Kartik Madhukar Patil)

This is to certify that the above statement made by the candidate is correct to the best of my/our knowledge.

Prof. Anand Parey

Dr. Krishna Mohan Kumar

Mr. Kartik Madhukar Patil has successfully given his M.Tech. Oral Examination held on **May 23, 2025**.

Signature(s) of Supervisor(s) of M.Tech. thesis

Date: 17-06-2025

Convener, DPGC

Date: 20-06-2025

ACKNOWLEDGEMENTS

Above all, I would like to thank God for the life experiences, accomplishments, and failures that have shaped me into the person I am today. My sincere gratitude goes to my parents and siblings for their love, affection, and belief in me.

The entire M. Tech. program has been a valuable experience for me, not only in terms of acquiring skills in the field of noise control, but also in terms of learning a lot more about research methods, positive attitude towards life, and interpersonal relationships.

I thank my supervisors, **Prof. Anand Parey** and **Dr. Krishna Mohan Kumar**, for encouraging me to harness the best out of me. I thank them for providing me an opportunity to work in the Noise Vibration Harshness (NVH) Lab and Theoretical and Applied Acoustics Lab (TAAL) at IIT Indore. They provided valuable suggestions to carry out the research work in a very systematic way. I also thank my M. Tech. thesis committee members: Dr. Indrasen Singh and Dr. Mayank Chouksey for providing valuable suggestions, constructive criticism, encouraging words. And all of it has given me a purpose to work hard with enthusiasm. To me, all of you have been outstanding teachers, mentors, and role models.

I also want to thank Mr. Santosh Yadav (Ph.D. scholar, NVH Lab) and Mr. Gaurav Sharma (Ph.D. scholar, TAAL Lab), Mr. Asif Nisar (MS Research Scholar, TAAL Lab) for helping me throughout my whole M. Tech. journey at IIT Indore.

My journey as a M. Tech. student at IIT Indore would not have been the same without my classmates. Everyday activities, politically incorrect jokes and, probably most significantly, our frequent after-works help make our division the greatest at IIT Indore. This work would not have been possible without the unending support of my parents, who helped me get to where I am now. My gratitude also extends to all lab colleagues, whose assistance has been priceless and has made working in the lab one of the most appealing aspects of my M. Tech. studies.

Thanks a lot, everyone...!

KARTIK PATIL

Dedicated to my family for their love, care, and blessings...!

Abstract

Drone belongs to class of Unmanned Aerial Vehicle (UAV) that have good manoeuvring abilities in both hovering as well as cruising operations. Because of these capabilities, the drone industry has experienced significant growth in both militaries as well civilian purposes. Their versatility and numerous applications have driven an ever-growing demand, and several companies are in the process of transforming urban transport by lifting it to the skies. Nevertheless, this progress has created increasing concerns regarding noise pollution, mainly due to the fact that drones fly at relatively low heights and also remain in close proximity to densely populated urban areas. Therefore, in order to use drones on the same scale as conventional vehicle for transportation as well as many other civilian and military purposes, it is necessary to mitigate the noise generated by drones.

This work presents the “Noise mitigation of drone” by making modifications in the geometry of propeller particularly by introducing serrations on the trailing edge of propeller. In the initial phase of work, through experimental noise measurement in semi-anechoic chamber, it is proved that propeller is the major source of noise in drones. CAD model baseline 1045 propeller is made in Siemens NX CAD software and prototype is made using resin 3D printer. Two types of serrations, namely single wavelength and double wavelength serrations are introduced on the trailing edge of propeller in CAD model and their prototype is made using resin 3D printer. Acoustic performance of the baseline and modified propellers is then compared by measuring their noise signatures in semi-anechoic chamber using ISO 3745 standard. The effect of these modifications on the aerodynamic performance of propeller is then studied by comparing the thrust force values of single and double wavelength serrated propellers with baseline propeller experimentally.

TABLE OF CONTENTS

LIST OF FIGURES.....	x
LIST OF TABLES	Error! Bookmark not defined.
ACRONYMS	xii
Chapter 1	1
1.1 Overview	1
1.2 Effect of Drone Noise.....	1
1.3 Sources of Noise in Drones	3
1.4 Noise Modelling for Propeller.....	4
1.5 Noise Control Strategy	5
1.6 Thesis outline:	6
Chapter 2	8
2.1 Previous Literature	8
2.2 Objectives of Study	11
Chapter 3	12
3.1 ISO STANDARD 3745	12
3.2 Microphone Positions for noise measurement.....	12
3.3 Experimental Setup	13
3.5 RESULTS	16
3.5.1 Sound Pressure Level Spectrum.....	16
3.5.2 Overall Sound Pressure Level (OASPL) comparison.....	17
Chapter 4	19
4.1 Baseline 3D printed propeller.....	19
4.2 Implementation of Noise Mitigation Strategy	19
4.2.1 With Single Propeller Working	19
4.2.2 With All Four Propeller Working.....	25
Chapter 5	30
5.1 Thrust Measurement Setup.....	30
5.2 Thrust Measurement Results	31
Chapter 6	32
6.1 Introduction	32
6.2 Conclusions	32
6.3 Recommendation for Future Work.....	33
References	34

LIST OF FIGURES

Fig. 1. 1: Applications of Drones	1
Fig. 1. 2: Effects of Drone noise	2
Fig. 1. 3: Sources of Noise for Propeller.....	3
Fig. 1. 4: Geometrical Features of an Owl Wing	6
Fig. 2. 1: Geometrical Parameters of Serration tooth	8
Fig. 2. 2: Different cases of Serrated Trailing Edges.....	9
Fig. 2. 3: Double Wavelength Serrated Leading Edge	10
Fig. 2. 4: Comparison of Sound Power Level between Single and Double Wavelength Serrated Leading Edge	10
Fig. 3. 1: Top view of Microphone positions.....	13
Fig. 3. 2: Front View of Microphone positions	13
Fig. 3. 3: Semi-anechoic chamber	14
Fig. 3. 4: Interior View of Semi-anechoic chamber with noise measurement setup ...	14
Fig. 3. 5: Digital laser tachometer.....	15
Fig. 3. 6: Sound Pressure Level Spectrum (dB) with Std. Baseline propeller and with only motor at microphone position 1 for 100% throttle condition.....	16
Fig. 3. 7 Sound Pressure Level Spectrum (dBA) with Std. Baseline propeller and with only motor at microphone position 1 for 100% throttle condition.....	17
Fig. 3. 8: OASPL at different microphone locations in dB and dBA at 100% throttle condition.....	18
Fig. 4. 1 : CAD model of Baseline Propeller.....	19
Fig. 4. 2: Baseline 3D printed propeller.....	19
Fig. 4. 3: Single Wavelength Serrated Propeller	20
Fig. 4. 4: Propeller with Dimple on its surface	20
Fig. 4. 5: Comparison of SPL for Baseline and Serrated propeller with Dimples at Mic1 location and 50% throttle condition	21
Fig. 4. 6: Comparison of OASPL at different microphone locations for 15 % throttle conditions	21
Fig. 4. 7: Comparison of OASPL at different microphone locations for 35 % throttle conditions	22

Fig. 4. 8: Comparison of OASPL at different microphone locations for 50 % throttle conditions	23
Fig. 4. 9: Comparison of Average Sound Pressure Level (SPL) for different cases of propellers and throttle conditions.....	23
Fig. 4. 10: Comparison of Sound Power Level (SWL) at different microphone locations for different cases of propellers and different throttle conditions	24
Fig. 4. 11: Single Wavelength Serrated Propeller.....	25
Fig. 4. 12: Double Wavelength Serrated Propeller	25
Fig. 4. 13: Comparison of SPL for Baseline, Single Wavelength and Double Wavelength Serrated propeller at Mic1 location and 50% throttle condition	26
Fig. 4. 14: Comparison of OASPL at different microphone locations for 15 % throttle conditions	26
Fig. 4. 15: Comparison of OASPL at different microphone locations for 35 % throttle conditions	27
Fig. 4. 16: OASPL comparison at different microphone locations for 50 % throttle conditions	27
Fig. 4. 17: Comparison of Average Sound Pressure Level (SPL) for different cases of propellers and throttle conditions	28
Fig. 4. 18: Comparison of Sound Power Level (SWL) at different microphone locations for different cases of propellers and different throttle conditions	29
Fig. 5. 1: Thrust Measurement Setup.....	30
Fig. 5. 2: Thrust force comparison for different cases of propeller and for different throttle conditions	31

ACRONYMS

UAV	Unmanned Aerial Vehicle
BPF	Blade Passing Frequency
FWH	Ffwoes-Williams/Hawkings Equation
ISO	International Organization for Standardization
SPL	Sound Pressure Level
OASPL	OverAll Sound Pressure Level
SWL	Sound Power Level
CAD	Computer Aided Design
dB	Decibel
Hz	Hertz

Chapter 1

Introduction

1.1 Overview

Sound is a type of energy that propagates in waves through a medium which is elastic, like air. Sound is produced when the pressure changes make particles in the medium move back and forth and produce wave motion. The waves transport the pressure changes from the source and reach the ear, where they are sensed and transmitted to the brain, where they are perceived as sound [1].

Noise, in contrast, is any sound that is undesirable—either because it is of high intensity or because of its unpleasant nature. What is acceptable or pleasant to one is annoying or disruptive to another. Persistent or extreme exposure to noise will result in hearing damage, compromising communication skills and possibly other health problems. The severity of adverse effects rises with increasing levels and longer exposure to noise [1].

1.2 Effect of Drone Noise



Fig. 1. 1: Applications of Drones [3]

Drones, or unmanned aerial vehicles (UAVs), have gained widespread popularity in recent years with their multitude of uses. Once designed for use in the military, drones are now commonly used in applications like aerial photography, surveillance,

agriculture, inspection of infrastructure, and package delivery. Their potential to visit hard-to-reach places, act independently, and minimize manned operations have placed them at the centre of commercial and civil operations. With increasing urban air mobility and use of drones, concerns about their environmental impact on noise pollution specifically have come into focus.

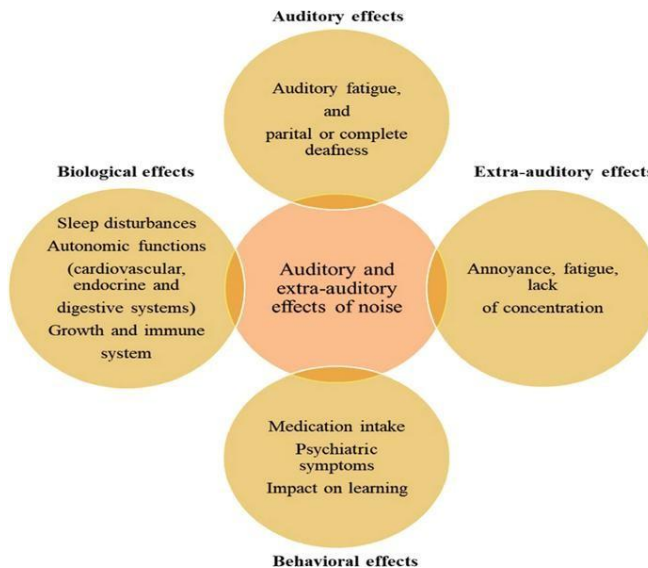


Fig. 1. 2: Effects of Drone noise

Noise from drones, especially because it is high-pitched and variable, has the potential to cause a variety of extra-auditory as well as auditory effects on human health. Auditory effects involve auditory fatigue and, in severe or long-lasting cases, partial or total loss of hearing. The effects of drone noise go far beyond hearing, though. Non-auditory effects like annoyance, mental fatigue, and decreased concentration are widely reported, particularly when drones fly over residential or urban environments. These interferences greatly impact everyday activities and overall quality of life.

Biological noise exposure effects include sleep interference and disturbance of autonomic processes such as cardiovascular, endocrine, and gastrointestinal systems. Chronic exposure can also degrade immune function and impact growth, especially in vulnerable populations like children and the elderly. Drone noise also induces behavioural effects, including enhanced medication dependency, psychiatric symptoms such as anxiety or irritability, and impaired ability to learn. These effects underscore the importance of taking noise pollution seriously as a public health issue in the context of expanding drone activity. To address these impacts, the innovation of less noisy

propeller technologies as well as working regulation policies are necessary, particularly with drone use expanding in both commercial and civilian airspace.

1.3 Sources of Noise in Drones

Drones have two main sources of noise, namely propeller and electric motor on which propeller is mounted. In current work, experimentally it is proved that propeller is the major source of noise and hence, if we want to reduce overall noise of drone, it is necessary to mitigate propeller noise.

The noise emitted by drone propeller is again divided into two components in frequency domain as tonal component and broadband component of noise. Hence, the pressure fluctuations radiated from propeller blades in far field are divided into two parts as

$$\mathbf{P}' = \mathbf{P}'_{TN} + \mathbf{P}'_{BB} \quad (1.1)$$

The tonal noise is generated due to periodic cutting of air column as propeller rotates. When we convert the pressure fluctuations data from time domain to frequency, we can see these sharp tonal components of noise at frequency known as Blade Passing Frequency (BPF) and its harmonics which is given by

$$BPF = \frac{RPM \text{ of Propeller} \times \text{No. of Blades}}{60} \quad (1.2)$$

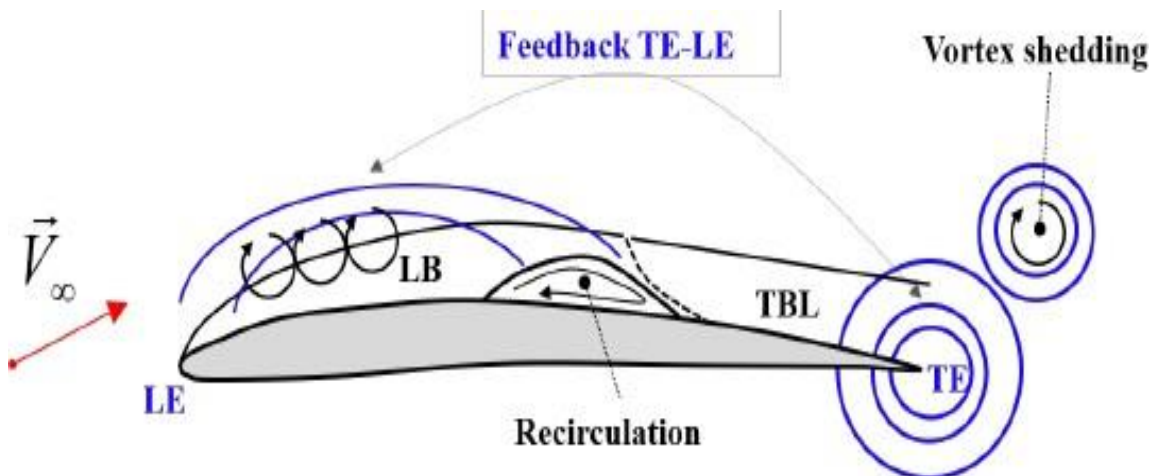


Fig. 1. 3: Sources of Noise for Propeller [9]

The broadband component of noise on the other hand is generated due to

1. Interaction of incoming turbulent flow with propeller leading edge

2. Transition of boundary layer from laminar to turbulent at trailing edge of propeller
3. Irregular flow separation from propeller surface
4. Blade Vortex Interaction i.e. interaction of vortices shed from trailing edge of one blade with leading edge of another blade
5. Blade Wake Interaction i.e. interaction of wake generated by trailing edge of one blade with leading edge of succeeding blade

1.4 Noise Modelling for Propeller

The noise radiated by propellers can be predicted from solution of non-homogeneous wave equation known as Ffwoes-Williams/Hawkings (FWH) [9] equation given by

$$\frac{1}{a^2} \cdot \frac{\partial^2(P')}{\partial t^2} - \frac{\partial^2(P')}{\partial x_i^2} = \frac{\partial^2 T_{ij}}{\partial x_i \cdot \partial x_j} + \frac{\partial}{\partial t} \{ \rho_a \cdot v_i \cdot \delta(f) \cdot \frac{\partial f}{\partial x_i} \} - \nabla \{ \Delta p_{ij} \cdot \delta(f) \cdot \frac{\partial f}{\partial x_i} \} \quad (1.3)$$

Where:

a: Speed of sound

P': Pressure perturbation

t: Observer time

x_i : Position vector components in i^{th} direction

T_{ij} : Lighthill stress tensor components

ρ_a : Air density

v_i : Velocity components in i^{th} direction

$\delta(f)$: Dirac delta function

f: Surface function defining body surface radiating pressure waves

Δp_{ij} : Pressure fluctuations on source body surface

The right-hand side of FWH equation has three source terms each representing different type of noise source. The first term is quadrupole type of source representing sound produced due to pressure fluctuations caused by turbulent structures in flow. It consists of components of Lighthill stress tensor [9] which is given by

$$T_{ij} = \rho v_i v_j + ((p - p_o) - c_o^2(p - p_o)) \delta_{ij} - \tau_{ij} \quad (1.4)$$

In above equation, first term represents Reynolds stress which accounts for pressure fluctuations due to velocity fluctuations in flow, second term accounts for compressibility effects and third term represents viscous stress tensor that accounts for dissipation of sound energy due to viscous effects.

The second source term of FWH equation is monopole type of source representing sound produced due to volume displacement as propeller rotates. The third term is dipole type of source and represents sound produced due to fluctuations of pressure on propeller surfaces as the lift and drag force of propeller are not constant. The Dirac delta function ($\delta(f)$) from second and third terms ensures that contributions from these terms are non-zero only for surface defined by $f = 0$ and gradient of surface function defining body surface scales these contributions depending on direction of flow and orientation of propeller surface.

1.5 Noise Control Strategy

For control of any noise source, there are two basic principles which are followed as follows

1. Control at Source i.e. modifying the source in such a way that it produces less noise
2. Control in Path i.e. by damping the energy of sound waves e.g. by designing some kind of enclosure

In current work, the ‘Control at Source’ principle of noise control is used i.e. the propeller, which is major source of noise in drones is modified in such a way that it makes less noise. For reducing propeller noise, inspiration is taken from nature particularly from wings of owl as they are one of the most silent predators in nature. The wings of owl three main geometrical features as shown in fig. 4 which are

1. Comb made from stiff feathers on leading edge of wing
2. Fringes made of flexible filaments on trailing edge of wings
3. Soft down coating on the suction surface of wing

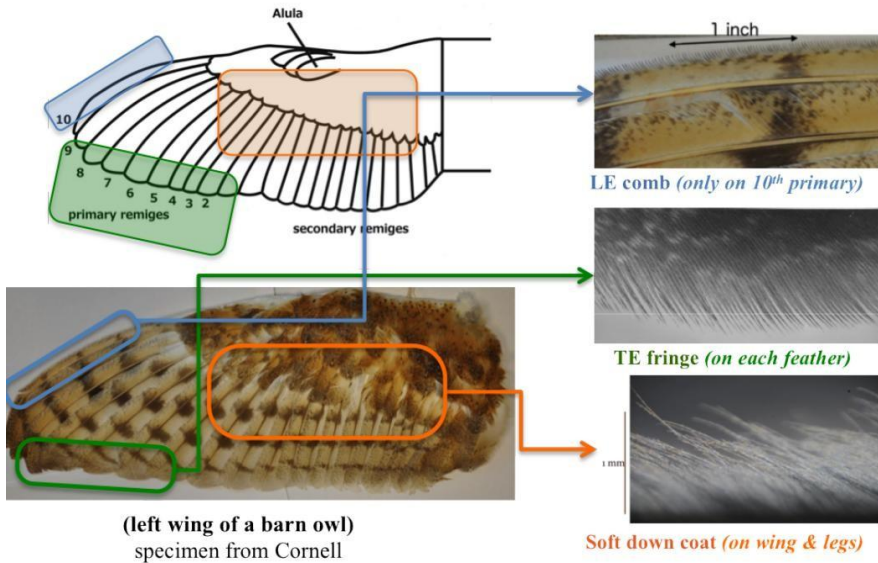


Fig. 1. 4: Geometrical Features of an Owl Wing [5]

These geometrical features create destructive interference between pressure fluctuations generated by air flowing over the surface of owl's wing which is responsible for their silent flight. By implementing these geometric features on drone propeller, thus it may be possible to reduce its noise.

1.6 Thesis outline:

Current research work is carried out according to sequence described below and is divided into 5 chapters as follows:

Chapter 2. Literature review: Reviews the previous research available for the noise control of drones, how the noise control strategies are implemented for drone propellers and their effect on the overall acoustic as well as aerodynamic performance of drone propellers

Chapter 3. Experimental Measurement of Standard 1045 propeller Noise:

Explains the experimental setup for the measurement of drone noise in semi-anechoic chamber as per ISO 3745 standard and the results of noise measurement in terms of

SPL spectrum, OASPL, average SPL and Sound Power Level bar plots for standard 1045 propeller

Chapter 4. Baseline 3D Printed Propeller and Noise Mitigation Strategy: Briefly explains the 3D printed propeller that is taken as baseline propeller for further study. Further, explains the implementation of different noise control strategies for propeller and the acoustic performance of modified propellers is compared with that of baseline propeller experimentally and the results are shown in terms of SPL spectrum, OASPL, average SPL and Sound Power Level bar plots.

Chapter 5. Experimental Measurement of Propeller Thrust: Explains the experimental setup for thrust measurement of propeller, the effect of noise control strategies on thrust of propeller is then represented by comparing the thrust force of modified propellers with that of baseline propeller.

Chapter 6. Conclusions and Scope of Future Work: This chapter examines the objectives of given project, explains summary of the results obtained and provides recommendations for future work that may improve acoustic as well as aerodynamic performance of propeller.

Chapter 2

Literature Review

2.1 Previous Literature

Over the past few years, considerable progress made with small-scale unmanned aerial vehicles (UAVs) has raised increasing concern about their acoustic effect, especially in populated or noise sensitive environments. Propeller induced sound has been found to be the leading source of UAV noise among numerous sources of UAV noise, particularly in electric multi-rotors. The noise is largely caused by aerodynamic interactions, such as unsteady vortices and blade-wake interactions, which create tonal and broadband components.

To mitigate this noise, various methods have been employed. These include geometric optimization of blade profiles like varying the twist angle, chord length and pitch of propeller. Some researchers have also employed the use of flexible low noise materials for reducing the propeller noise. Amongst these, a promising and biologically inspired method has been found by studying the silent flight of owl. Owls are known for their silent flight because they have specific features such as combed leading edges, serrated trailing edges and velvet-like surfaces which disrupt the coherent vortex formation and delay the transition of boundary layer from laminar to turbulent over their wing surface which helps in reducing their noise [9].

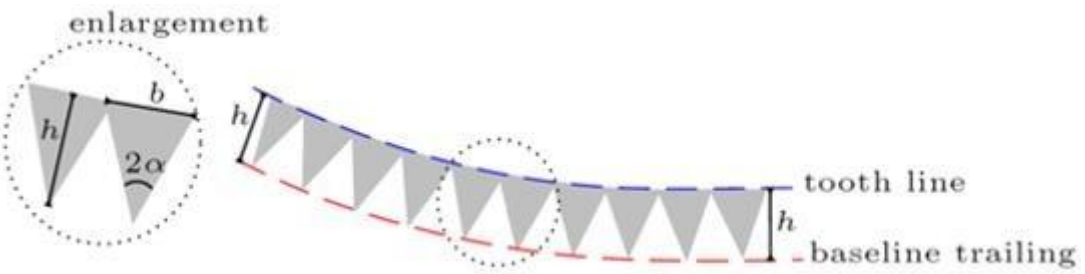


Fig. 2. 1: Geometrical Parameters of Serration tooth [10]

Inspired by these biological features, researchers have investigated the application of serrated trailing edges to aerofoils and propeller blades. Theoretical work by Howe [4,5] provided the basis into how sawtooth serrated edges modify the vortices shade from trailing edge and decrease noise radiation. Using these serrated trailing edges, significant reduction in noise can be obtained if following two conditions are met

1. The serration angle (2α) should be smaller than 45° .
2. The aspect ratio ($2b/h$) of serrat tooth should not be greater than 4.

Paolo et. al. [10] in his study applied noise control method of serrations and studied experimentally the effect of geometrical parameters like serrat height and serrat width on reduction obtained by creating 23 different configurations of propeller by varying the height and width of serrat tooth for hovering and advanced flight cases by using wind tunnel system in an anechoic chamber through microphone measurements. From his study, best results were obtained when the serrat height and width was kept at 8 mm and 6 mm which corresponds to aspect ratio of 1.5. Thus, he concluded that the noise reduction obtained using serrations increases with increase in tooth height till certain height after which again noise reduction decreases.

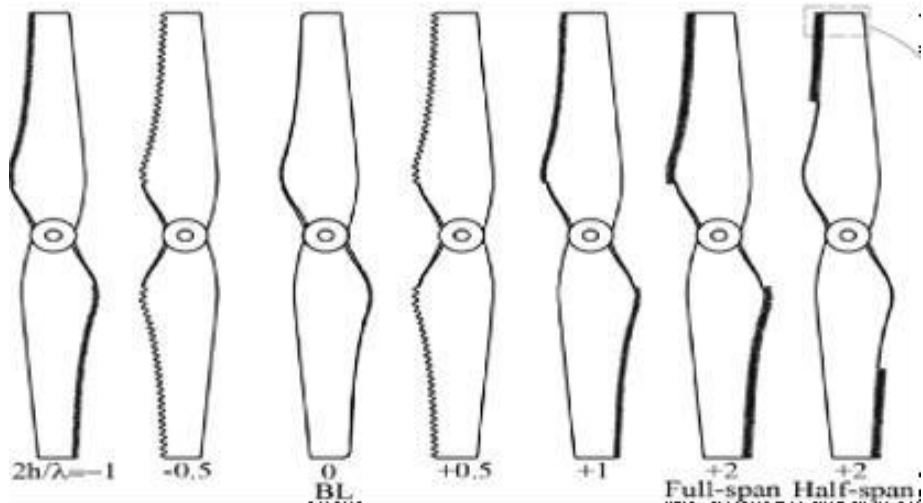


Fig. 2. 2: Different cases of Serrated Trailing Edges [5]

Yannian et. al [6] compared different designs of trailing edges serrations by varying the height to wavelength ($2h/\lambda$), the way in which serrations are made i.e. cut-in and add-on serrations also the radial range of serrated teeth on trailing edge from aerodynamic as well as acoustic performance perspective for case of forward flight through microphone and balance measurement in an anechoic chamber. All serrat design were found effective in reducing the propeller noise. The propellers with add-on serrations were found more effective than cut-in serrated propeller. The propeller having add-on serrations with height to wavelength ratio ($2h/\lambda$) of 0.5 were found best from both acoustic as well as aerodynamic perspective giving considerable reduction of approximately 2 dB in OASPL. Also, propellers with serrations till half-length

serrations performed approximately the as full-length serrated propellers in terms of their acoustic performance.

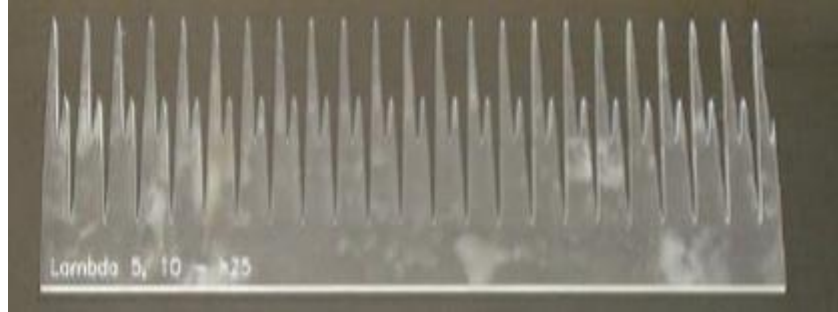


Fig. 2. 3: Double Wavelength Serrated Leading Edge

P. Chaitanya. et. al. [8] experimentally studied the effect of double wavelength serrations i.e. the serrations obtained by combining the two single wavelength components on acoustic performance of airfoils and compared the noise reduction obtained with double wavelength serrations with the noise reduction obtained with single wavelength components individually through microphone measurements in an anechoic chamber having wind tunnel facility.

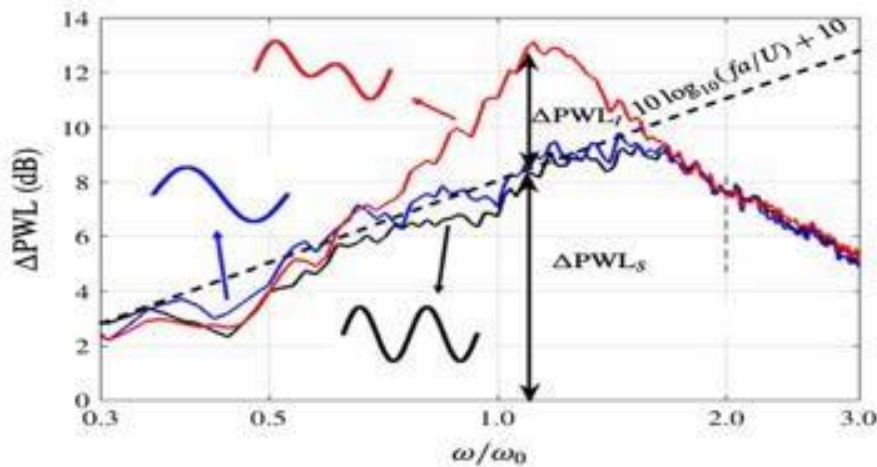


Fig. 2. 4: Comparison of Sound Power Level between Single and Double Wavelength Serrated Leading Edge

From experimental measurement, considerable reduction in noise is obtained using double wavelength serrations as compared to their single wavelength counterparts giving approximately 4 dB of more reduction in sound power level as shown in fig. 2.4.

2.2 Objectives of Study

- To reduce the noise of drone propellers without affecting their maximum thrust.
- To experimentally study the effect of single and double wavelength serrations on noise and thrust produced by drone propeller.

Chapter 3

Experimental Measurement of Standard 1045 Propeller

Noise

3.1 ISO STANDARD 3745

To estimate the sound power level or sound energy level produced by the noise source, ISO 3745 provides techniques for measuring the SPL (sound pressure levels) on a measurement surface enclosing a noise source in anechoic and semi-anechoic rooms. It provides specifications for the testing environment and equipment as well as methods for obtaining the surface sound pressure level, which is used to determine the sound power level. A device, machine, component, sub-assembly might be the noise source, the radius of hemispherical measurement surface is dependent on the size of source as well as placement of the source. The methods given in this International Standard require the source to be mounted in either an anechoic room or a hemi-anechoic room having specified acoustic characteristics. The methods are then based on the premise that the sound power or sound energy of the source is directly proportional to the mean-square sound pressure over a hypothetical measurement surface enclosing the source and otherwise depends on the physical constants of air. [2]

Spherical measurement surface:

The spherical measurement surface shall be centred on the acoustic centre of the noise source under test, either the actual acoustic centre if known or an assumed acoustic centre such as the geometric centre of the source.

Hemispherical measurement surface:

The hemispherical measurement surface shall be centred on a point on the floor of the test room vertically beneath the assumed acoustic centre of the noise source under test, either the actual acoustic centre if known, or the geometric centre if the acoustic centre is unknown.

3.2 Microphone Positions for noise measurement

According to ISO 3745, Fig. 3.1 shows the Top view of microphone positions which gives idea of distance of each microphone positions from noise source on the floor, microphone positions '2', '5', '9' covers the exhaust air flow region. Figure 3.3 shows

the Front view which gives idea about the height of the microphone at positions shown in Figure 3.2.

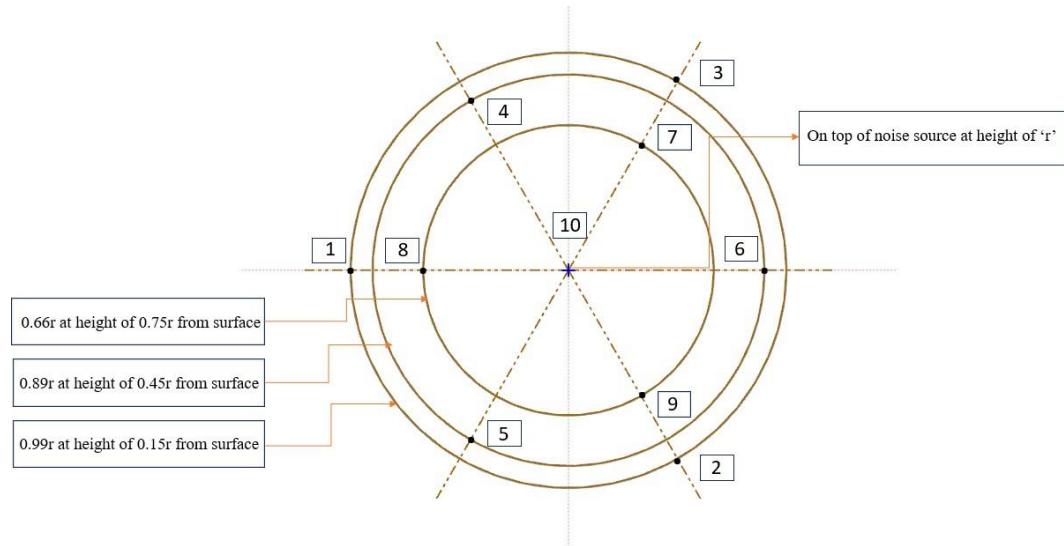


Fig. 3. 1: Top view of Microphone positions

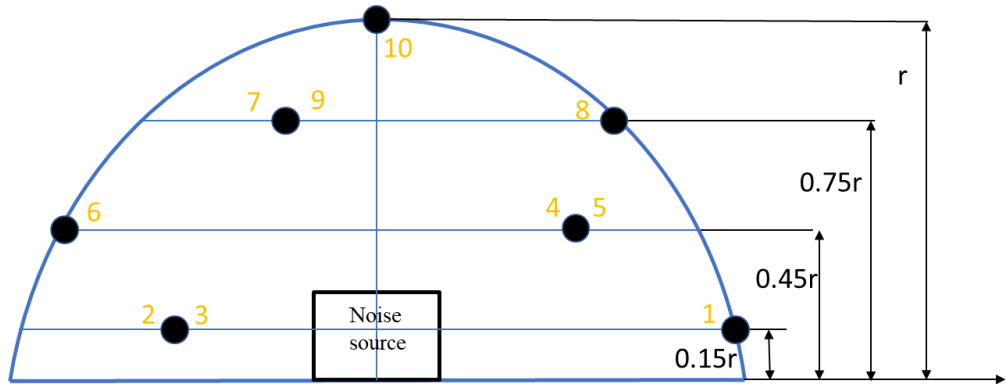


Fig. 3. 2: Front View of Microphone positions

3.3 Experimental Setup

Fig. 3.3 shows the interior of semi anechoic chamber with experimental setup marked by numbers as follows

1. GRAS 46AE free field microphone
2. Drone with baseline 1045 propeller with base frame
3. Laptop with NV Gate software
4. OR34 Data Acquisition System (DAQ)



Fig. 3. 3: Semi-anechoic chamber

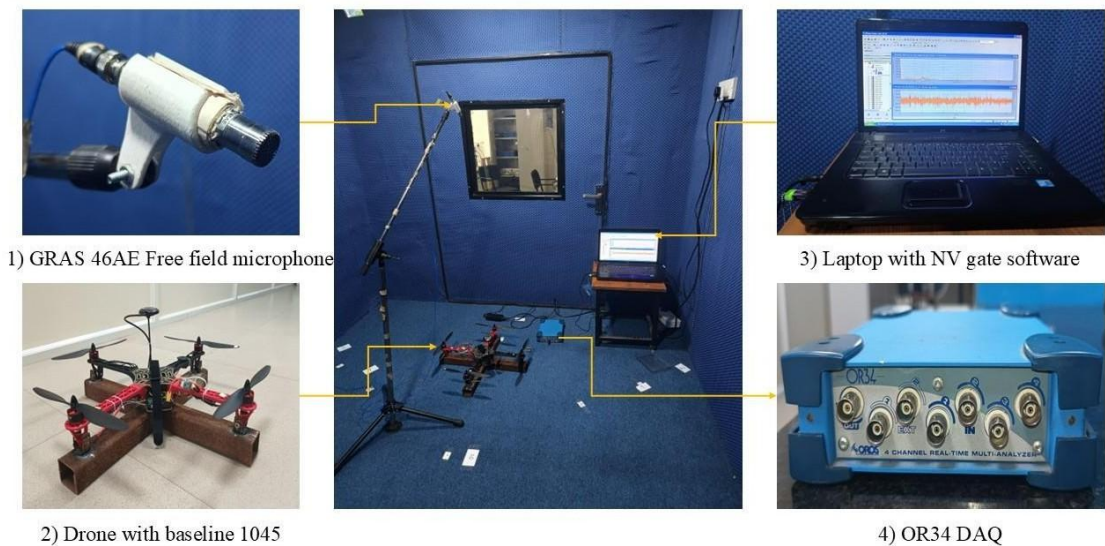


Fig. 3. 4: Interior View of Semi-anechoic chamber with noise measurement setup

In the current work, noise measurement for drone has been done according to ISO 3745 standard in semi anechoic chamber shown in fig. 3.4 as it creates free field condition for noise measurement for two cases of drone:

1. When only one motor of drone is operational
2. When all the motors of drone are operational

For first case, the centre of operational motor is kept at the centre of hemispherical dome and radius is taken as 1 m and all the vertical distances of microphone positions are increased by 14 cm to consider the height of the base plate attached to drone to keep it stationary during measurement. For second case, since there are 4 noise sources (4 propellers), the centre of drone frame is kept at the centre of hemi-spherical dome and the radius of hemi-spherical dome is taken as 1.28 m to consider the length of arms of drone. The noise data was captured at sampling frequency of 12.8 kHz for sampling time of 10 sec. The rotational speed of propeller is measured using MEXTECH DT-2236C digital laser tachometer. The noise measurement is done for following different cases of drone

1. With only 4 motors
2. With both 4 baseline 1045 propellers and motors
3. With single 3D printed propeller and motor
 - i. Baseline 1045 propeller
 - ii. Single Wavelength Serrated Propeller
4. With all 4 3D printed propellers
 - i. Baseline 1045 propeller
 - ii. Single Wavelength serrated propellers
 - iii. Double Wavelength serrated propellers



Fig. 3. 5: Digital laser tachometer

3.4 RESULTS

3.4.1 Sound Pressure Level Spectrum

Sound pressure level (SPL) is a logarithmic measure of sound relative to reference pressure and represents the variation of sound pressure with frequency.

$$SPL = 10 * \log \left(\frac{P}{P_{ref}} \right) \quad (3.1)$$

$$P_{ref} = 2 * 10^{-5} \text{ Pa}$$

Fig. 3.6 shows variation of SPL in dB with frequency at microphone position 1 for two cases of drone: one with only motor and one with both propeller and motor to find out the contribution of motor noise from overall noise of the drone for 100% throttle condition. From SPL spectrum, we can see sharp peaks at 267.5 Hz, 534.37 Hz and 802.5 Hz which occur due to periodic cutting of air column at blade passing frequencies and its harmonics. These peaks also known as tonal noise are dominant components of drone noise and addressing these peaks is crucial to mitigate the drone noise. Similarly, the variation of SPL spectrum with frequency is plotted for all 10 microphone locations.

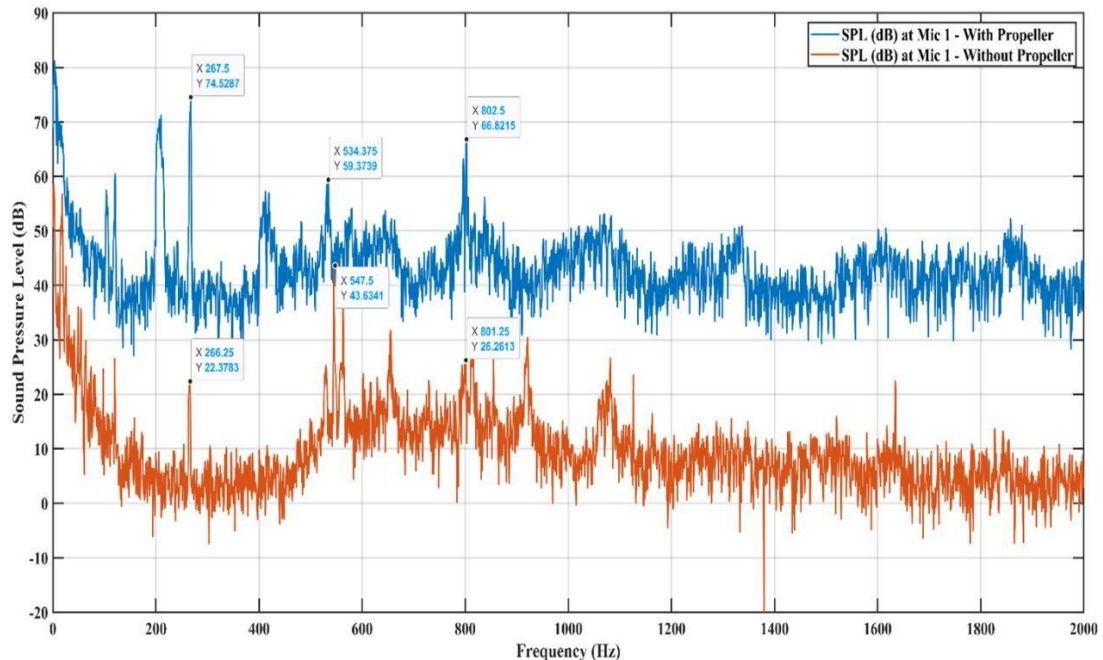


Fig. 3.6: Sound Pressure Level Spectrum (dB) with Std. Baseline propeller and with only motor at microphone position 1 for 100% throttle condition

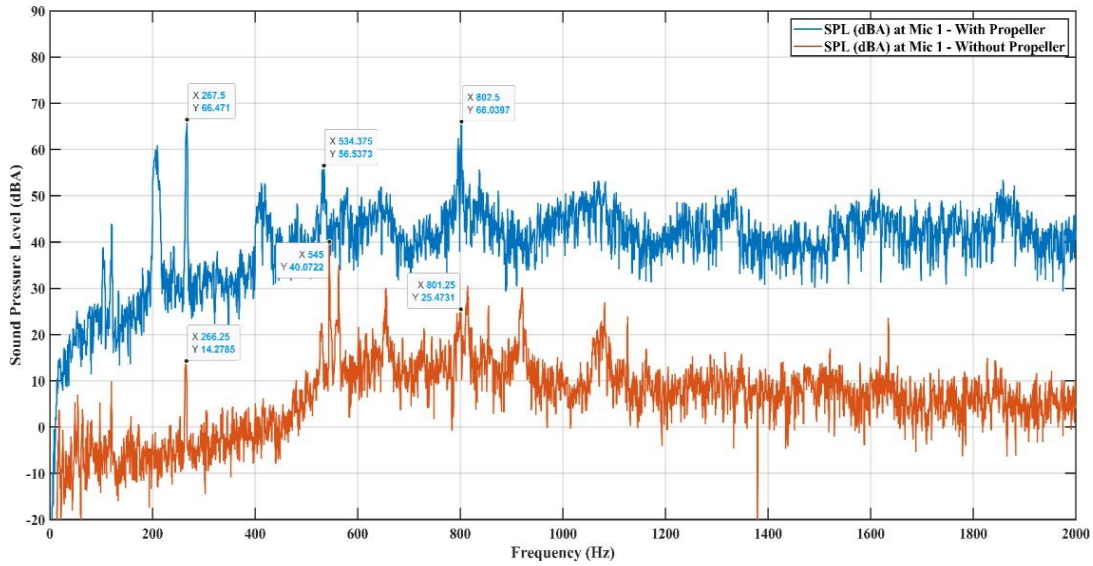


Fig. 3. 7 Sound Pressure Level Spectrum (dBA) with Std. Baseline propeller and with only motor at microphone position 1 for 100% throttle condition

The human ear responds differently to sounds of different frequencies. Extensive audiological surveys have resulted in weighting factors for different purposes, however the A- weighting network is now used exclusively in most measurement standards and the mandatory noise limits. Fig. 3.7 shows the SPL spectrum for two cases of drone: first with both propeller and motor and second with only motor in dBA respectively. It can be observed from the Fig. 3.7, after applying A-weighting correction factor, SPL before 200 Hz i.e., in lower frequency get affected significantly.

3.4.2 Overall Sound Pressure Level (OASPL) comparison

Overall Sound Pressure Level (OASPL) is the single value representation of total acoustic energy contained in a sound signal across the entire frequency range and can be obtained by logarithmically adding the SPL values at individual frequency points as per following formula

$$OASPL = 10 \log(\sum_{i=1}^n 10^{0.1L_{p,i}}) \quad (3.2)$$

Where, $L_{p,i}$ represents the SPL value at i^{th} frequency point. Using above formula, OASPL is calculated for 10 microphone positions as per ISO 3745 standard for two cases of drone: one with only motor and second with both motor and standard baseline 1045 propeller and is represented in the form of bar plot in dB and dBA as shown in fig. 3.8. From fig. 3.8 it can be observed that, the OASPL of only motor lies between 66dB and 74dB and between 45dBA and 49dBA. The OASPL for the case of both

propeller and motor lies between 90 dB and 103 dB and between 80 dBA and 90 dBA. The logarithmic average SPL for both the cases are 86.71 dBA and 47.95 dBA, respectively having a difference of approximately 40 dB. Hence, we can conclude that propellers are major sources of noise in the case of drones.

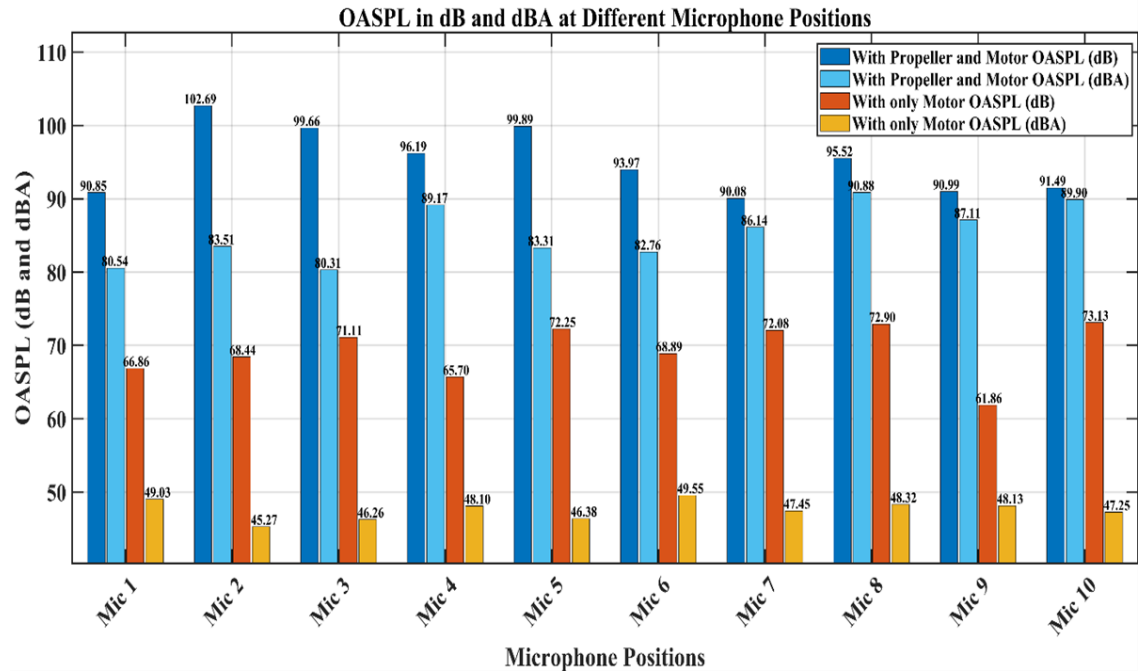


Fig. 3. 8: OASPL at different microphone locations in dB and dBA at 100% throttle condition

Chapter 4

Baseline 3D printed propeller and Noise mitigation Strategy

4.1 Baseline 3D printed propeller



Fig. 4. 1 : CAD model of Baseline Propeller

Fig. 4.1 shows the CAD model of propeller which is considered as baseline propeller for further study made using Siemens NX CAD software. The geometric modifications for noise reduction can be directly made in the cad model and the prototype of propeller can be made using resin 3D printer.



Fig. 4. 2: Baseline 3D printed propeller

Fig. 4.2 shows the baseline 3D propeller printed using Sonic Mighty Resin 3D printed made of Aqua 8k 3D printing resin.

4.2 Implementation of Noise Mitigation Strategy

4.2.1 With Single Propeller Working

In current work, the inspiration for noise mitigation strategy is taken from wings of owls as they are one of the most silent predators in nature. The wings of owls have geometrical features like serrations on their leading and trailing edges of wings and soft downy coating on the wing's suction surface which create destructive interference between pressure fluctuations produced by flow structures convecting along the wing surface. Hence, in current work, initially two strategies are tested as follows

1. Serrated Trailing Edge



Fig. 4. 3: Single Wavelength Serrated Propeller

2. Dimples on the propeller surface



Fig. 4. 4: Propeller with Dimple on its surface

The effect of the above two strategies is tested initially by operating the drone with single propeller working and using the same experimental setup as described in the previous chapter in the semi-anechoic chamber for following four cases

1. Baseline propeller with dimples
2. Baseline propeller with smooth surface
3. Serrated propeller with dimples
4. Serrated propeller with smooth surface

The above four cases are repeated for 3 throttle conditions as follows

1. 15% throttle (3780 rpm)
2. 35% throttle (5280 rpm)
3. 50% throttle (6600 rpm)

Then OASPL, average SPL and Sound Power Level (SWL) bar plots are compared to determine which noise control strategy is more effective.

4.2.1.1 Sound Pressure Level (SPL) Spectrum

From SPL spectrum comparison of baseline and single wavelength serrated propeller, sharp peaks are observed at approximately 220 Hz and its harmonics, which represents the Blade Passing Frequency (BPF) as propeller rotates at approximately 6600 rpm for 50% throttle condition when the drone is operated with one propeller operational. From SPL spectrum, we can see that both tonal and broadband components of noise are less for serrated propeller as compared to baseline propeller.

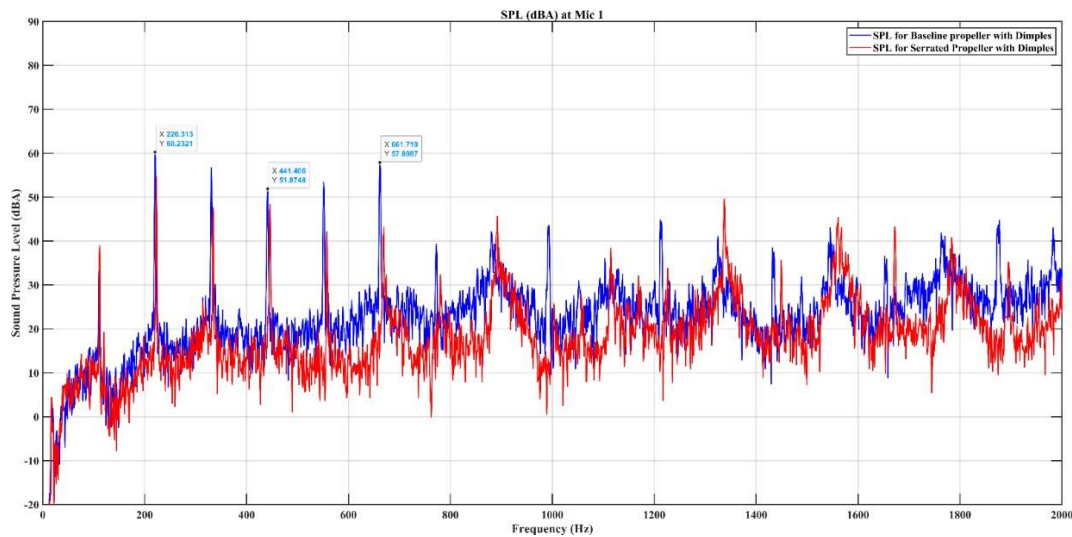


Fig. 4. 5: Comparison of SPL for Baseline and Serrated propeller with Dimples at Mic1 location and 50% throttle condition

4.2.1.2 Overall Sound Pressure Level (OASPL) comparison

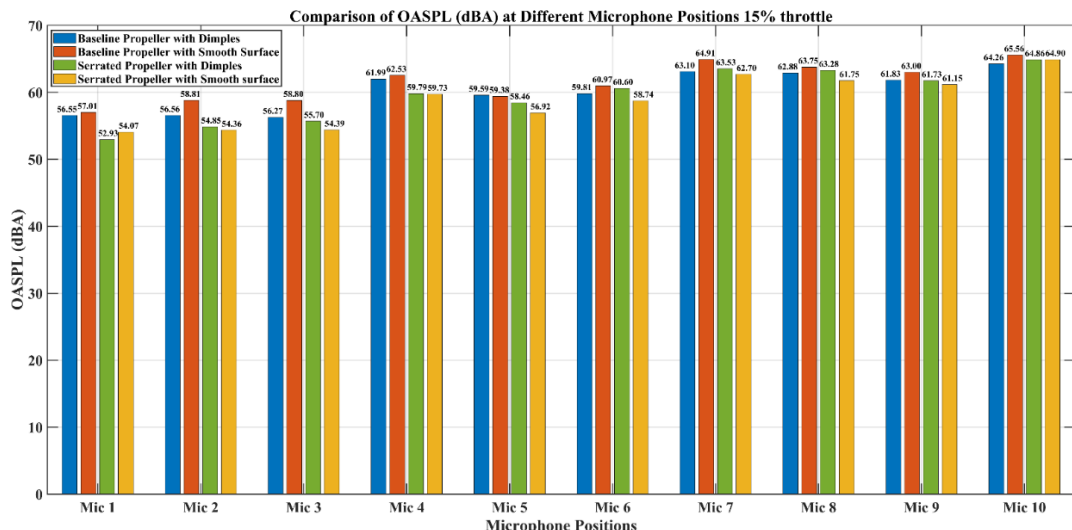


Fig. 4. 6: Comparison of OASPL at different microphone locations for 15 % throttle conditions

Noise measurement has been performed for the above four cases of propeller and for 3 throttle conditions and using logarithmic addition formula of SPL, OASPL value is calculated for 10 microphone positions and is shown in the form of bar plot.

From fig. 4.6 it is observed that, OASPL for the case of baseline propeller with smooth surface is highest at all the microphone position except at mic 5 location and it is highest at mic 10 location having value of 65.56 dBA and both noise control strategies are effective in reducing noise produced by propeller but the noise reduction obtained with different strategies is different at different microphone locations.

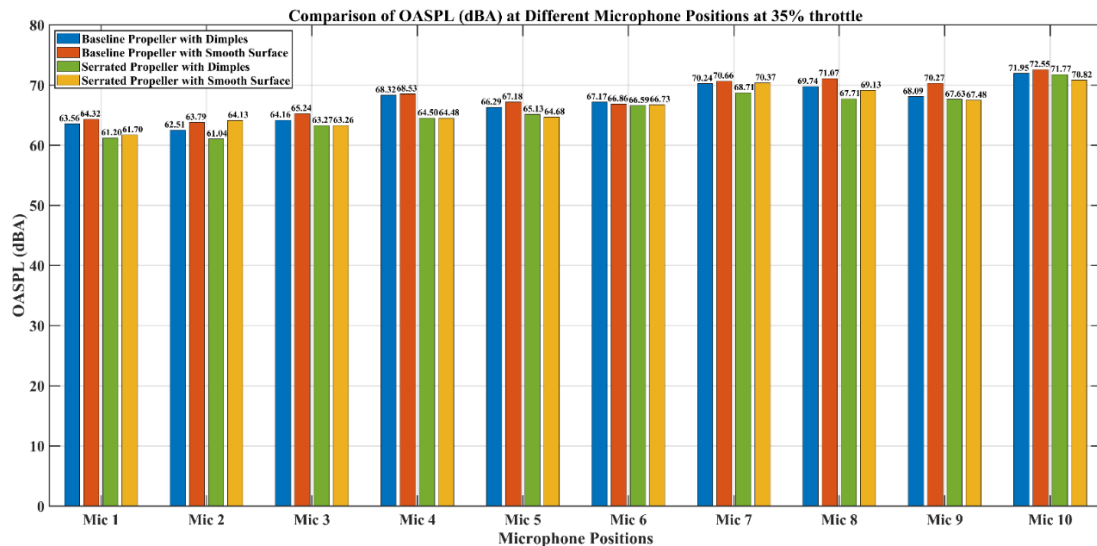


Fig. 4. 7: Comparison of OASPL at different microphone locations for 35 % throttle conditions

From fig. 4.7, similar trend is observed with OASPL values at 35% throttle conditions for all cases of propeller. The OASPL value is highest for baseline propeller with smooth surface for all microphone positions except at position 6 but again a definite pattern is not observed in noise reduction using the noise control strategies of serration and dimple on propeller surface.

From fig. 4.8 again similar trends are observed. The OASPL for baseline propeller with smooth surface is highest for all microphone locations except at mic 4 and mic 7 where OASPL for baseline propeller with dimples on its surface and at mic 8 location for serrated propeller with dimples on its surface.

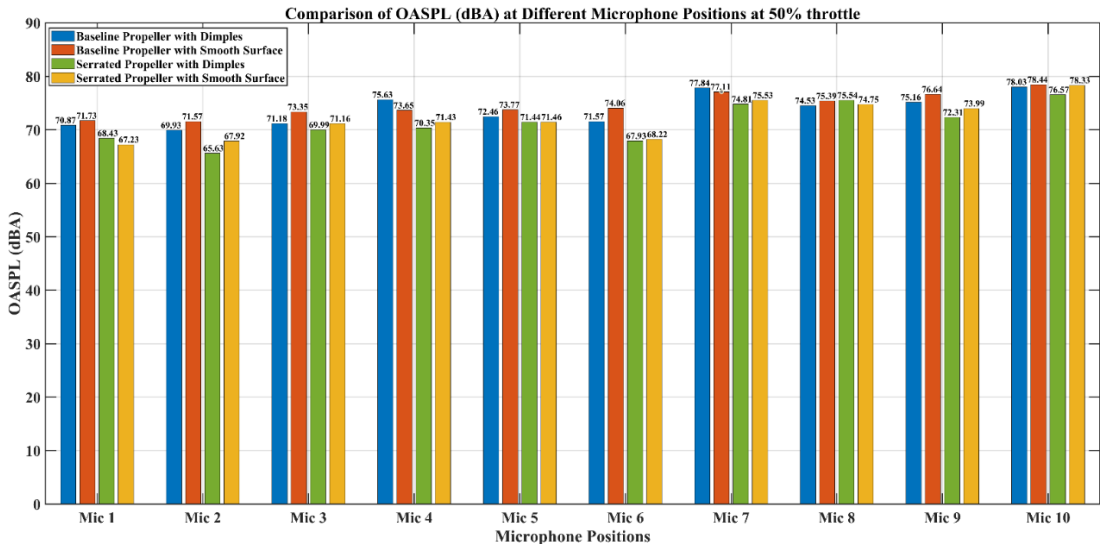


Fig. 4. 8: Comparison of OASPL at different microphone locations for 50 % throttle conditions

4.2.1.3 Average Sound Pressure Level (SPL) comparison

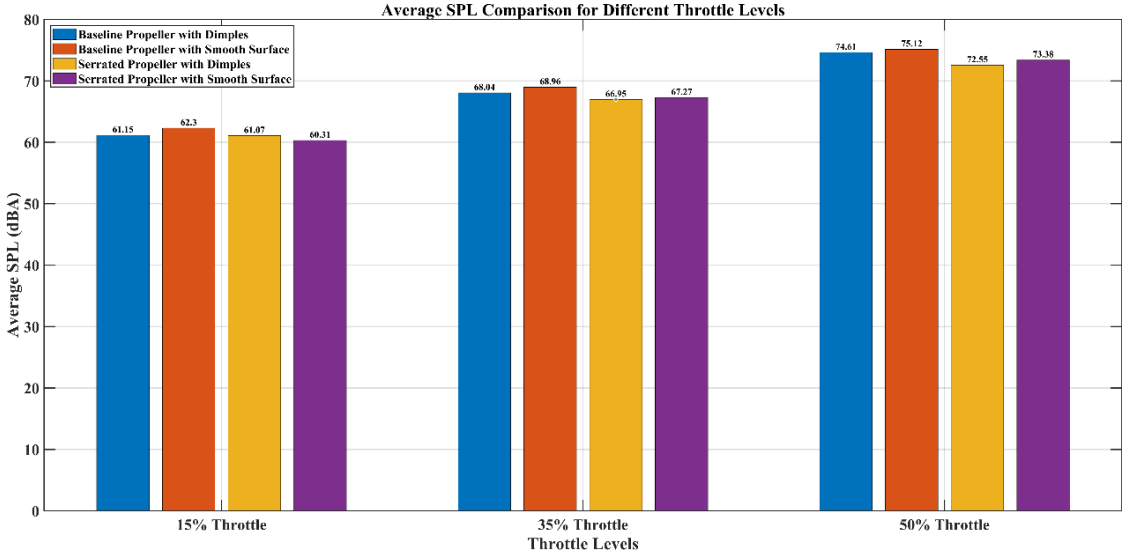


Fig. 4. 9: Comparison of Average Sound Pressure Level (SPL) for different cases of propellers and throttle conditions

To quantify the overall effect of noise control strategies and to find out which strategy is most effective, average SPL is calculated using logarithmic averaging formula from OASPL values at 10 microphone locations for four cases of propeller and for 3 different throttle conditions and is represented in the form of bar plot as shown in fig. 4.9. From average SPL comparison, it is observed that the average SPL is highest for baseline propeller with smooth surface and both noise control strategies are effective in reducing

noise of propeller. At 15% throttle condition, the noise reduction obtained is relatively less, but as throttle increases the noise reduction obtained also increases particularly for the case of serrated propeller with dimples on its surface. At 35% throttle condition, noise reduction obtained is approximately 2.01 dB and at 50% throttle condition, approximately 2.57 dB respectively. Thus, we can say that the effectiveness of noise control strategies increases with increase in throttle i.e. rotational speed of propellers.

4.2.1.4 Sound Power Comparison (SWL)

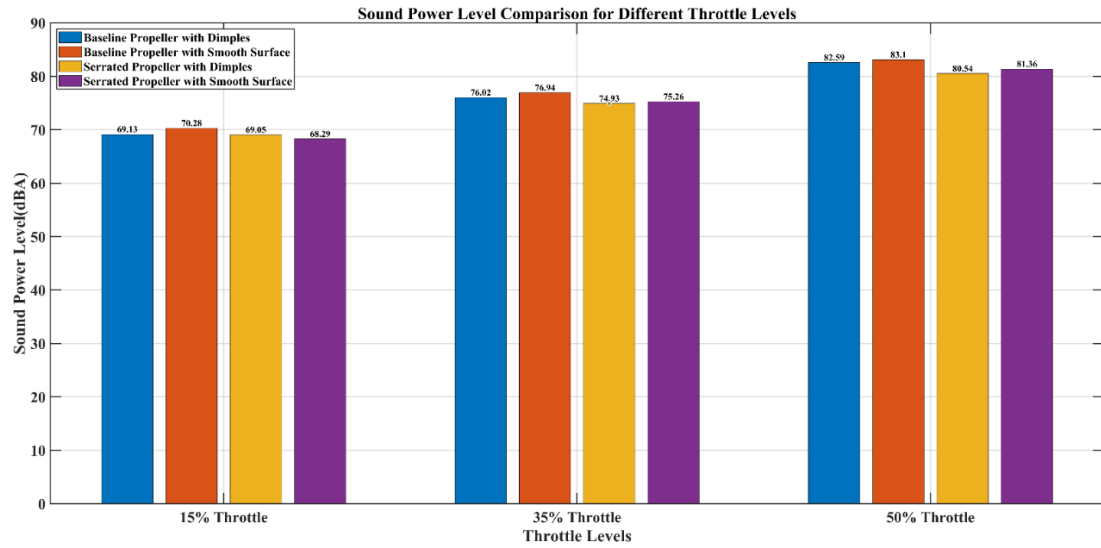


Fig. 4. 10: Comparison of Sound Power Level (SWL) at different microphone locations for different cases of propellers and different throttle conditions

Sound power level (SWL) is inherent property of sound source and logarithmic measure of the total acoustic energy emitted by source per unit time and is independent of the environment or the distance from the source. The Sound Power Level is calculated from average SPL using following formula

$$SWL = SPL_{avg} + 10 \log_{10} S_m \quad (4.1)$$

Where, S_m represents surface area of imaginary hemispherical dome on which noise measurement is done at 10 different locations as per ISO 3745 standard and is given by

$$S_m = 2\pi r^2 \quad (4.2)$$

Where, r represents radius of imaginary hemispherical dome.

Thus, SWL is basically average SPL plus a constant which represents measurement surface area. Hence, the same trend is observed with SWL as average SPL. The SWL

value is highest for baseline propeller with smooth surface and reduction in SWL increases with increase in throttle i.e. rotational speed of propeller.

4.2.2 With All Four Propeller Working

After testing the effect of single wavelength serrations and dimples on propeller surface on the noise produced by propeller, it is observed that serrations are more effective in reducing propeller noise as compared to dimples. So, in upcoming part, serrations are taken as final noise control strategy with two variations of serrations i.e. single and double wavelength serrations, respectively. The effect of these two types of serrations on propeller noise is tested by operating the drone with all its four-propeller working and by taking noise readings according to same noise measurement setup as explained earlier in semi-anechoic chamber as per ISO 3745 standard.

1. Single Wavelength Serrations



Fig. 4. 11: Single Wavelength Serrated Propeller

2. Double Wavelength Serrations



Fig. 4. 12: Double Wavelength Serrated Propeller

The above two cases of propeller are tested for three throttle conditions

1. 15% throttle (2695 rpm)
2. 35% throttle (2695 rpm)
3. 50% throttle (4260 rpm)

4.2.2.1 Sound Pressure Level Spectrum

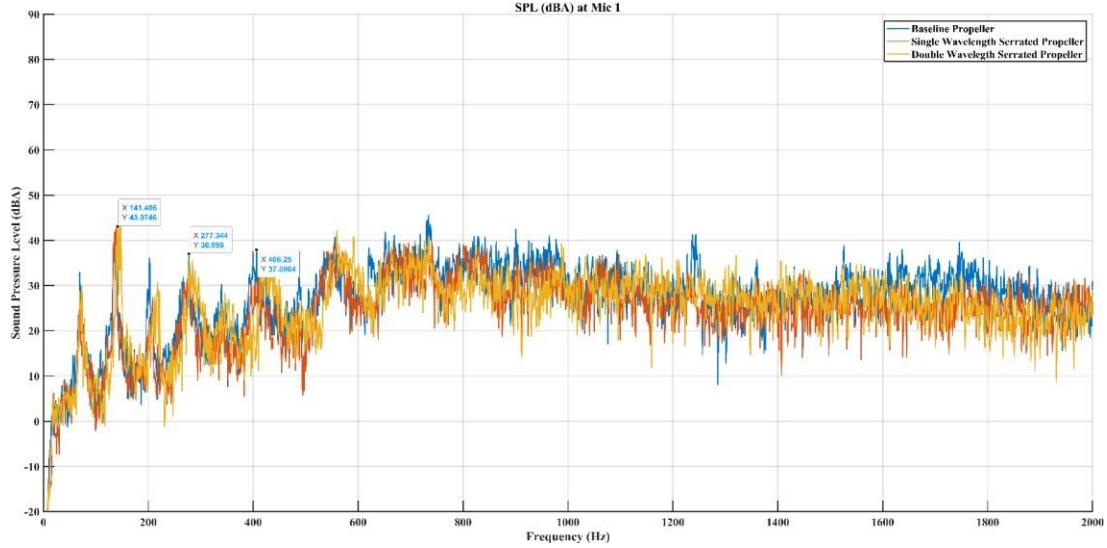


Fig. 4. 13: Comparison of SPL for Baseline, Single Wavelength and Double Wavelength Serrated propeller at Mic 1 location and 50% throttle condition

From fig. 4.13, sharp peaks can be observed at 141 Hz and its harmonics which represent tonal component of noise for propeller rotating at 50% throttle i.e. 4260 rpm conditions. From fig. 4.13, it is observed that the tonal and broadband components of noise for baseline propeller are more as compared to single and double wavelength serrated propeller.

4.2.2.2 Overall Sound Pressure Level (OASPL) spectrum

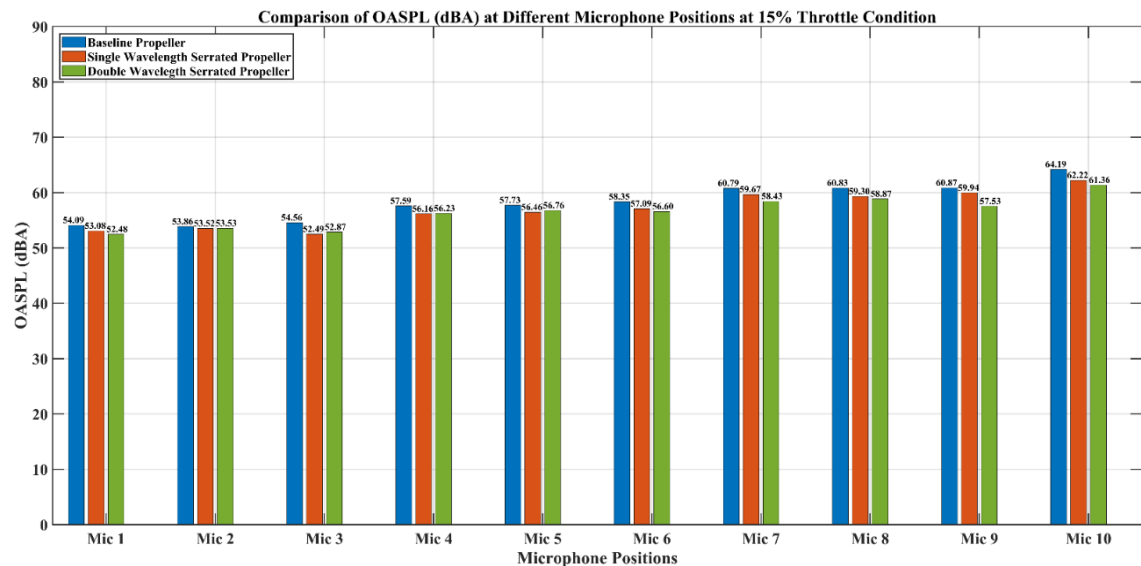


Fig. 4. 14: Comparison of OASPL at different microphone locations for 15 % throttle conditions

From fig. 4.14, it is observed that the OASPL of baseline propeller is more as compared to single and double wavelength serrated propellers. Also, it is observed that for mic 1 to mic 5 location, the single wavelength serrations are giving more noise reduction as compared to double wavelength serrated propeller. But from mic 6 to mic 10, double wavelength serrations are more effective in reducing propeller noise.

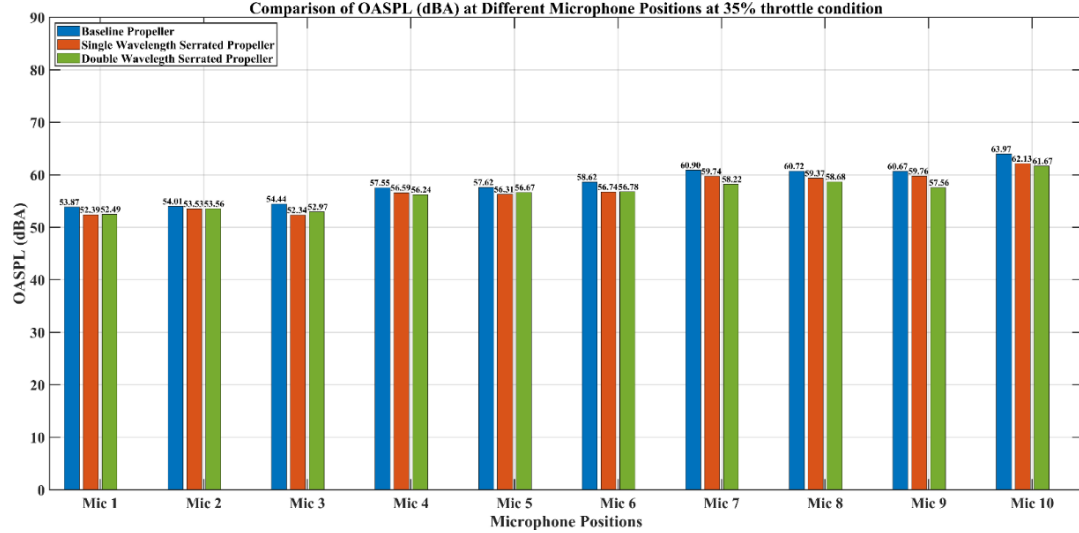


Fig. 4. 15: Comparison of OASPL at different microphone locations for 35 % throttle conditions

When the drone is operated with all four of its propellers working, the rotational speed of propeller is same for 15% and 35% throttle condition, hence the OASPL values for both cases are almost same as we can see from fig. 4.14 and fig. 4.15 and same trend, we can observe for both cases.

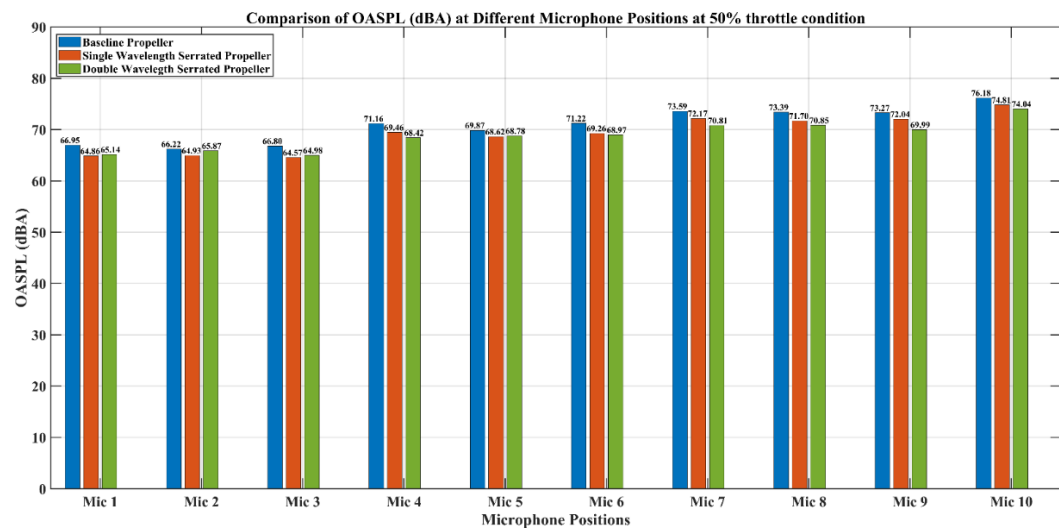


Fig. 4. 16: OASPL comparison at different microphone locations for 50 % throttle conditions

From fig. 4.16, again same trend is observed as 15% and 35% throttle conditions. For mic 1 to mic 5 locations, single wavelength serrations are more effective and for mic 6 to mic 10 locations, double wavelength serrations are more effective in reducing propeller noise.

4.2.2.3 Average Sound Pressure Level (SPL) Spectrum

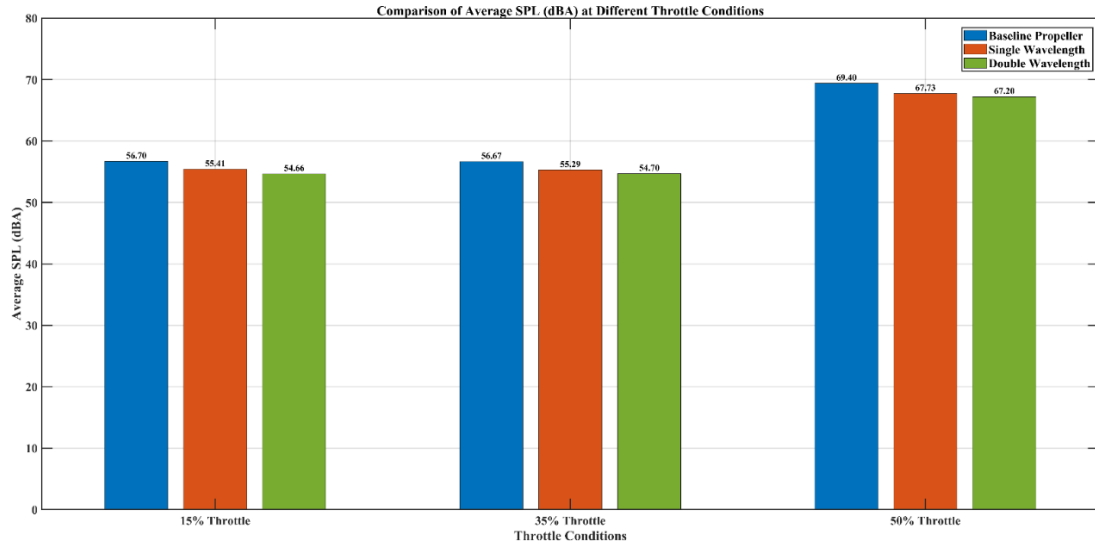


Fig. 4. 17: Comparison of Average Sound Pressure Level (SPL) for different cases of propellers and throttle conditions

To quantify the overall effect and to determine which serrations i.e. single wavelength or double wavelength serrations are more effective in reducing propeller noise, average SPL values are calculated by logarithmically averaging the OASPL values at 10 microphone locations and is represented in the form of bar plot as shown in fig. 4.17 for 3 different throttle conditions. From average SPL comparison, it is observed that both serrations are effective, but the effectiveness of serrations increases with increase in throttle i.e. rotational speed of propeller. Also, double wavelength serrations are more effective giving 2.19 dB of reduction whereas single wavelength serrations give 1.66 dB of reduction in average SPL at 50% throttle condition.

4.2.2.4 Sound Power Level (SWL)

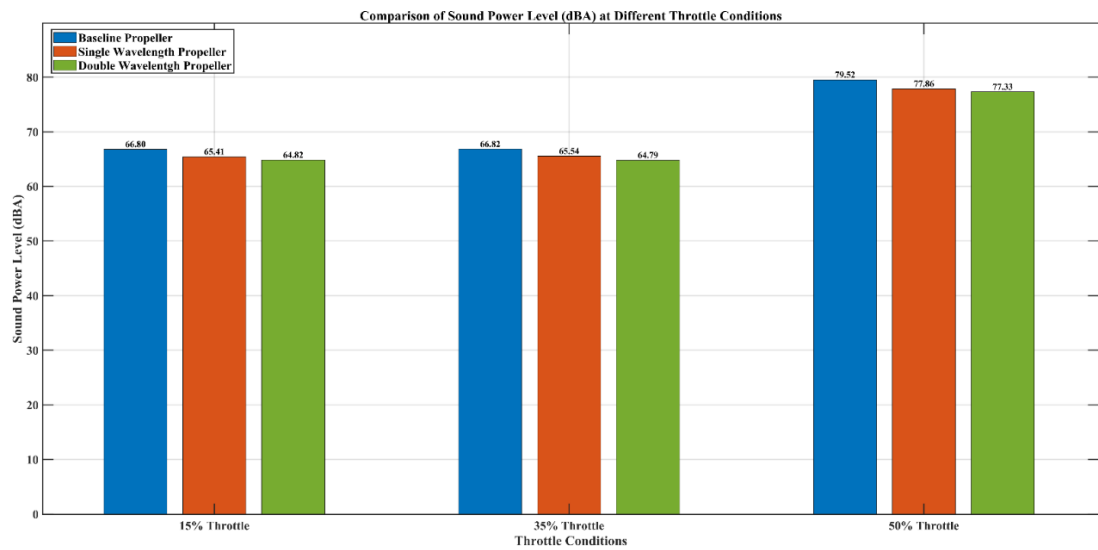


Fig. 4. 18: Comparison of Sound Power Level (SWL) at different microphone locations for different cases of propellers and different throttle conditions

Sound power level is since average SPL plus a constant, hence same trend is observed with Sound power level as well. Both serrations are effective in reducing the sound energy emitted by propeller, but double wavelength serrations are comparatively more effective as compared to single wavelength serrations.

Chapter 5

Thrust Measurement

5.1 Thrust Measurement Setup

The drone propeller has airfoil shape due to which when it rotates rapidly, it accelerates the air in downward direction creating a pressure difference between its upper and lower surfaces. Due to this pressure difference, an equal and opposite reaction is obtained as per Newton's 3rd law of motion which pushes the drone in upward direction.

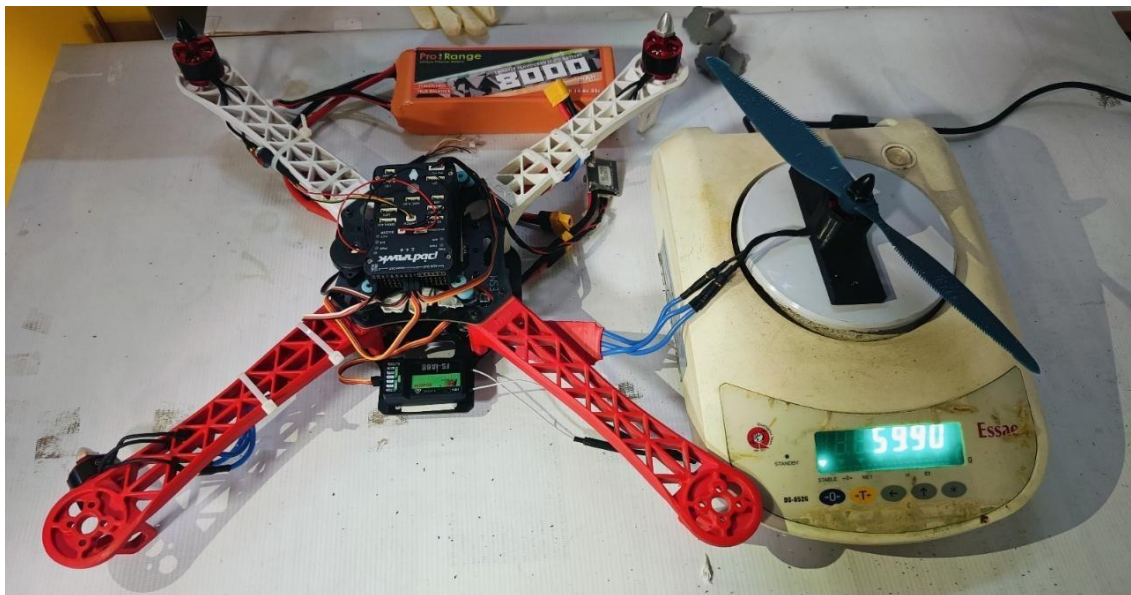


Fig. 5. 1: Thrust Measurement Setup

In current work, to measure the thrust of propeller, a single motor along with propeller is taken out from drone and it is mounted on the weighing machine Essac DS-852G which can give accurate readings till 0.01 g. The propeller is mounted on motor in reversed manner such that the suction surface of propeller is on lower side and the pressure surface of propeller is on upper side, and it is rotated in opposite direction i.e. clockwise propeller is rotated in anticlockwise direction. Due to this, as propeller rotates, the air will be pushed in upward direction and reaction force will be applied in a downward direction on the weighing machine and the thrust of propeller can be measured.

5.2 Thrust Measurement Results

Using the thrust measurement setup as explained earlier, the thrust of isolated propeller is measured for two throttle conditions as follows for the three cases of propeller i.e. baseline, single wavelength and double wavelength serrated propeller and is represented in the form of bar plot in fig.

1. 15% throttle (3780 rpm)
2. 35% throttle (5280 rpm)

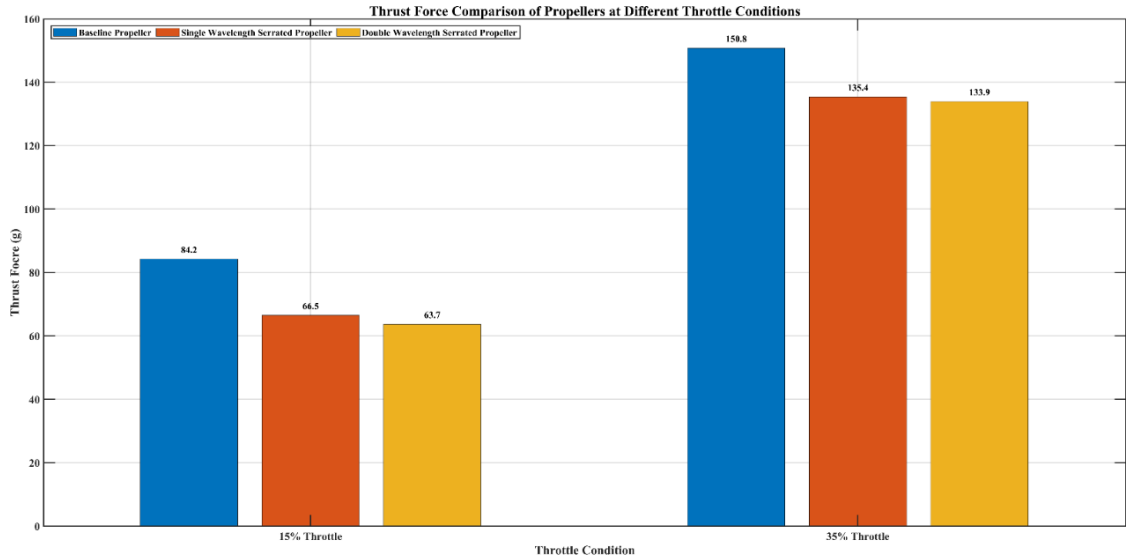


Fig. 5. 2: Thrust force comparison for different cases of propeller and for different throttle conditions

From fig. 5.2, reduction in thrust force produced by propeller is observed as serrations are introduced on its trailing edge due to reduction in effective surface area of propeller which produces thrust. This reduction is more for double wavelength serrations compared to single wavelength serrated propeller. But with increase in throttle i.e. rotational speed of propeller, this reduction in thrust also reduces as the reduction in thrust is 17.7 g and 20.5 g for single and double wavelength serrated propeller respectively at 15% throttle condition and 15.4 g and 16.9 g for single and double wavelength serrated propeller respectively at 35% throttle condition.

Chapter 6

6.1 Introduction

This chapter summarizes the present work study, comparison of propeller and motor noise, the effectiveness and comparison of two noise control strategies employed in current work i.e. serrated trailing edges and dimples on propeller surface, the comparison of noise reduction obtained using single and double wavelength serrations, the effect of serrations on thrust produced by propeller and recommendation for future work that can be done to improve the acoustic as well aerodynamic performance of drone propeller.

6.2 Conclusions

- Average SPLs of standard propeller and motor are 86.71 dBA and 47.95 dBA, respectively. Thus, we can conclude that the propeller is the main source of noise in drone.
- Both serrated trailing edges as well as dimple on propeller surface are effective in reducing the propeller noise but serrations are comparatively more effective in reducing propeller noise.
- Effectiveness of serrations in reducing noise of propeller increases with increase in throttle.
- When single propeller is working, approximately 2.51 dB of reduction in average SPL is obtained using single wavelength serrations as compared to baseline 3D printed propeller which correspond to approximately 25% reduction in acoustic pressure fluctuations produced by baseline 3D printed propeller at 50% throttle condition.
- When four propellers are working, approximately 1.66 dB and 2.19 dB of reduction in average SPL of propeller is obtained using single wavelength and double wavelength serrations which correspond to approximately 18.4% and 22.5% of reduction in acoustic pressure, respectively at 50% throttle condition
- Due to serrations, reduction in thrust produced by propeller is observed which is 10.21% for single wavelength propeller and 11.21% for double wavelength propeller.

6.3 Recommendation for Future Work

Although significant noise reduction can be obtained using serrations, they have the drawback of reducing the thrust force produced as shown in experimental measurement of thrust force. Future work can focus on the following areas:

- Serrations can be introduced on the leading edge of the propeller which from literature are observed to reduce noise as well as improve the thrust force produced by propeller.
- Parametric study can be done by varying the serration height and base width to optimize noise reduction obtained.
- Different combination of wavelength can be tested to create double wavelength serrations to optimize noise reduction obtained using them.
- Concept of metamaterials structures, i.e. creating textured pattern on the propeller surface to mimic geometrical features of owl's wings can be employed which have been known to reduce propeller noise without compromising with its thrust force

References

1. <https://iosh.com/health-and-safety-professionals>
2. <https://www.iso.org/standard/45362.html>.
3. <https://electricalfundablog.com/drones-unmanned-aerial-vehicles-uavs>
4. M. S. Howe; Noise produced by a sawtooth trailing edge. *J. Acoust. Soc. Am.* 1 July 1991; 90 (1): 482–487.
5. M.S. Howe, Aerodynamic noise of a serrated trailing edge, *Journal of Fluids and Structures*, Volume 5, Issue 1, 1991, Pages 33-45, ISSN 0889-9746,
6. Yannian Yang, Yong Wang, Yu Liu, Haitao Hu, Zhiyong Li, Noise reduction and aerodynamics of isolated multi-copter rotors with serrated trailing edges during forward flight, *Journal of Sound and Vibration*, Volume 489, 2020, 115688, ISSN 0022-460X.
7. Haitao Hu, Yannian Yang, Yu Liu, Xiaomin Liu, Yong Wang, Aerodynamic and aeroacoustic investigations of multi-copter rotors with leading edge serrations during forward flight, *Aerospace Science and Technology*, Volume 112, 2021, 106669, ISSN 1270-9638.
8. Chaitanya P, Joseph P, Narayanan S, et al. Performance and mechanism of sinusoidal leading-edge serrations for the reduction of turbulence–aerofoil interaction noise. *Journal of Fluid Mechanics*. 2017; 818:435-464.
9. Candeloro, Paolo, Daniele Ragni, and Tiziano Pagliaroli. 2022. "Small-Scale Rotor Aeroacoustics for Drone Propulsion: A Review of Noise Sources and Control Strategies" *Fluids* 7, no. 8: 279.
10. Candeloro, Paolo, et al. "Experimental Fluid Dynamic Characterization of Serrated Rotors for Drone Propulsion." *Journal of Physics: Conference Series*. Vol. 1977. No. 1. IOP Publishing, 2021.
11. Hasheminejad, Seyed Mohammad, et al. "Airfoil Self-Noise Reduction Using Fractal-Serrated Trailing Edge." 2018 AIAA/CEAS Aeroacoustics Conference. 2018.
12. Chaitanya P, Joseph P, Narayanan S, Kim JW. Aerofoil broadband noise reductions through double-wavelength leading-edge serrations: a new control concept. *Journal of Fluid Mechanics*. 2018; 855:131-151. doi:10.1017/jfm.2018.620

13. Lilley, G. (1998, June). A study of the silent flight of the owl. In 4th AIAA/CEAS aeroacoustics conference.
14. Yannian Yang, Yu Liu, Haitao Hu, Xiaomin Liu, Yong Wang, Elias J.G. Arcondoulis, Zhiyong Li, Experimental study on noise reduction of a wavy multi-copter rotor, *Applied Acoustics*, Volume 165, 2020, 107311, ISSN 0003-682X.
15. Jaron R., Moreau A., Guérin S., Schnell R., Optimization of trailing-edge serrations to reduce open-rotor tonal interaction noise (2018), *Journal of Fluids Engineering, Transactions of the ASME*, 140 (2), art. no. 021201.

